Analytical Methods

Accepted Manuscript

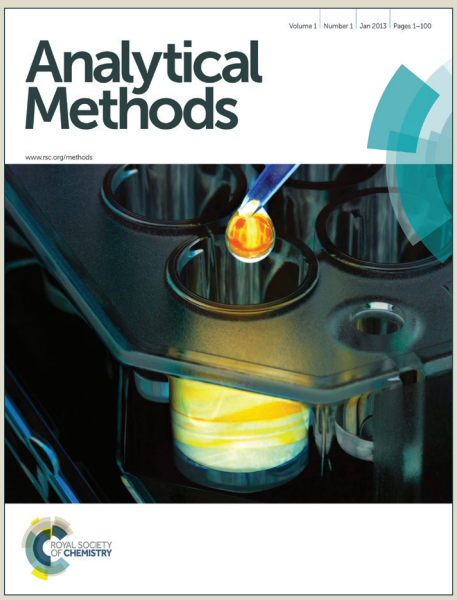

ROYAL SOCIETY OF CHEMISTRY

www.rsc.org/methods

Electrochemical sensor based on molecularly imprinted membranes on a *p*-ATP–AuNP modified electrode for the determination of acrylamide

Qiuyun Wang[1,3]; Jian Ji[1]; Donglei Jiang[1]; Yao Wang[3]; Yinzhi Zhang[1]; **Xiulan Sun**[1,2]

[1]State Key Laboratory of Food Science and Technology，[2]School of Food Science Synergetic Innovation Center Of Food Safety and Nutrition, Jiangnan University, Wuxi, Jiangsu 214122, China. [3]Wuxi higher health vocational technology school

Corresponding author: **Xiulan Sun**

Address: Jiangnan University, 1800 Lihu Avenue, Wuxi, Jiangsu 214122, China.

E-mail: sxlzzz@jiangnan.edu.cn; Tel: +86-510-85329015

Abstract:

A novel electrochemical sensor for acrylamide (AM) detection based on moleculary imprinted polymer (MIP) membranes was constructed. *p*-Aminothiophenol (P-ATP) and AM were assembled on the surface of a gold nanoparticle (AuNP) modified glass carbon electrode (GCE) by the formation of Au-S bonds and hydrogen-bonding interactions, and polymer membranes were formed by electropolymerization in a polymer solution containing *p*-ATP, $HAuCl_4$, tetrabutylammonium perchlorate (TBAP) and a dummy template molecule propanamide (PMA). A novel molecularly imprinted sensor (MIS) was obtained after the removal of PMA. Cyclic voltammetry (CV) and differential pulse voltammetry (DPV) measurements were used to monitor the electropolymerization process and its optimization, which was further characterized by scanning electron microscopy (SEM). The linear response range of the MIS was between 1×10^{-12} and 1×10^{-7} mol L^{-1}, with a detection limit of 0.5×10^{-12} mol L^{-1}. This research provides a fast, sensitive and real-time method for the detection of AM in a real sample without complex pretreatment and with average recoveries higher than 95 % and a relative standard deviation (RSD) lower than 3.73 %. All the obtained results indicate that the MIS is an effective electrochemical technique to determine AM in real-time and in a complicated matrix.

Keywords:

Electrochemical sensor, Moleculary imprinted polymer, Acrylamide, Glass carbon electrode

1. Introduction

In 2002 the Swedish National Food Administration (SNFA) and the University of Stockholm together announced that certain foods that are processed or cooked at high temperature contain relatively high levels of acrylamide (AM). Since then the AM content in food, especially in fried or baked food, has attracted worldwide attention [1, 2]. Numerous analytical methods have been developed over the past few years to quantify AM in cooked food, water, and in biological fluids using gas chromatography with mass spectrometric detection (GC–MS) and high performance liquid chromatography after bromination or tandem mass spectrometric detection (LC–MS/MS) [3, 4]. To accurately determine AM levels in individual laboratories, a sensitive and selective analytical methodology that requires less expensive apparatus and direct analytical determination without complicated derivatization procedures is needed [5].

Molecular imprinting is a promising technique for the design of structured porous polymers having a precise arrangement of functional groups and template molecules [6, 7]. Electrochemical sensors and biosensors, which are also known as chemically and biologically modified electrodes, have been active areas of research in electroanalysis [8-10]. They are widely applied in many fields including health care [11], food safety [12], and in complex matrixes for medical [13], bioprocess control [14], and monitoring environments [15].

These sensors are cheap, able, highly selective and specific, and their high selectivity and specificity usually depend on a specific interaction between the analytes and a chemical matrix, which is known as the recognition element of the sensor [16, 17]. The sensitivity of an imprinted sensor is determined by the amount of effective recognition sites in the molecularly imprinted polymer films and their conductivity[18, 19]. Although the number of binding sites increases with an increase in the imprinted membrane's thickness, thick imprinted membranes can lead to the slow diffusion of analytes to recognition sites and inefficient communication between the imprinted sites and transducers[20, 21]. The polymerization of conductive polymers or doping with metal nanoparticles is the most effective way to improve the conductivity of molecularly imprinted sensors [22, 23]. The co-polymerization of gold nanoparticles (AuNP) and conductive polymers from the composite membrane results in high conductivity, a large specific surface area, and good biocompatibility[24-26].

In this study, a novel sensor for the determination of AM based on *p*-aminothiophenol (P–ATP) as a functional macromolecule and gold nanoparticles (AuNP) as a cross-linker was fabricated by surface imprinting using molecular imprinting technology [27]. It is known that AM can easily polymerize with other allyl monomers through its double bond and, therefore, the elution of AM from the molecularly imprinted polymer is difficult when it is used as a template molecule. As a result, a higher false positive reading is expected to give a detection result that is

too high. Therefore, its structural analogue propanamide (PMA), which is similar to AM in terms of its spatial structure, size, and functional groups, can be used as a dummy template molecule for the polymerization of MIPs [28, 29]. We hypothesized that a combination of surface molecular self-assembly and the co-polymerization of poly-aminothiophenol and gold nanoparticles (P–ATP–AuNP) on a Au electrode will produce a specific amount of effective imprinted sites and thus enhance its conductivity. The electrochemical behavior of AM at the imprinted film sensor was characterized by cyclic voltammetry (CV) and differential pulse voltammetry (DPV). The molecular imprinting sensor significantly improved the sensitivity and selectivity toward AM and also gave good repeatability. It can thus be potentially exploited for the detection of AM and its metabolites in biological assays. In addition, the sensor can be used to monitor non-electrochemical signal substances.

2. Experimental

2.1. Instruments and reagents

The morphology of the molecularly imprinted polymers (MIP) was observed using a scanning electron microscope (Hitachi S-4800, Japan). UV–vis spectra were obtained on an Arantes Avaspec-2048 UV–vis spectrophotometer with scanning wavelengths from 200 to 1100 nm. Cyclic voltammetry (CV), differential pulse voltammetry (DPV) and electrochemical impedance spectroscopy (EIS) were conducted using a CHI760C workstation (Chenhua, Shanghai, China), using a conventional three-electrode system in a solution containing 2.5×10^{-3} mol L^{-1} $Fe(CN)_6^{3-/4-}$ consisting of 0.0824 g $K_3Fe(CN)_6$, 0.1164 g $K_4Fe(CN)_6{\cdot}3H_2O$, and 0.1 M KCl. A glassy carbon electrode (GCE, Φ 3 mm) was used as the working electrode, a platinum wire was used as the auxiliary electrode and a saturated calomel electrode (SCE) was used as the reference electrode. Impedance spectra were recorded upon the application of bias potentials in a frequency range of 100 mHz to 10 kHz using an AC voltage of 5 mV in amplitude.

p-Aminothiophenol (P–ATP), tetrabutylammonium perchlorate (TBAP) and tetrachloroaurate (III) acid ($HAuCl_4$) were purchased from Sigma-Aldrich China, Inc.. Acrylamide (AM, 99.9%) and propionamide (PAM, 96%) were purchased from Shanghai Crystal Pure Industrial Co. Ltd. All the chemicals were HPLC analytical grade. Ultrapure water was used throughout this work. Standard solutions of AM were prepared in ethanol. Food samples were purchased from a local supermarket.

2.2. Pretreatment and self-assembly of glass carbon electrodes

A GCE was polished with alumina slurry (0.30 and 0.05 μm), rinsed thoroughly with doubly distilled water, and successively ultrasonicated in ethanol and doubly distilled water for 5 min. Cyclic voltammetry was performed in 0.5 mol L^{-1} H_2SO_4 solution over a potential range from −0.2 to 0.6 V (scan rate 100 mV s^{-1}). A GCE modified with AuNP was achieved using

electrodeposition in a de-aerated precursor solution of 0.5 mol L^{-1} H_2SO_4 containing 1×10^{-3} mol L^{-1} $HAuCl_4$ and a constant potential of -0.25 V was applied over an optimal time of 100 s[30]. P-ATP functionalized electrodes were prepared by immersing the AuNP modified GCE (AuNP/GCE) into a 2×10^{-2} mol L^{-1} P–ATP ethanol solution for 24 h at room temperature, and then washing the electrode thoroughly with ethanol and doubly distilled water to remove physically absorbed P–ATP [27]. The P–ATP modified AuNP/GCE was then immersed in an ethanol solution containing 1×10^{-3} mol L^{-1} PAM for 4 h. The electrode was removed and rinsed with ethanol and doubly distilled water to remove absorbed PAM, and then dried under nitrogen flow at room temperature.

2.3. Preparation of imprinted P–ATP–AuNP–PAM/Au modified GCE

P–ATP–AuNP–PAM/AuNP/GCE was immersed in an ethanol solution containing 1×10^{-2} mol L^{-1} P–ATP, 5×10^{-2} mol L^{-1} TBAP, 1×10^{-2} mol L^{-1} PAM and 0.2 g L^{-1} $HAuCl_4$. The co-polymerization was performed by the application of ten cyclic voltammetry cycles in an ice bath with a potential range from −0.3 to 1.2 V (scan rate 50 mV s^{-1})[27]. After electropolymerization, the composite membrane modified electrode was immersed in an ethanol:water (1:5) solution containing 0.5 mol L^{-1} H_2SO_4 for 300 s to remove the PAM template. The imprinted electrode was then rinsed with ethanol, doubly distilled water, and finally dried under nitrogen for further use.

We prepared a control electrode following the same procedure but without a template molecule. The control electrode was treated using the same procedure as for the imprinted electrode to ensure that any effects observed were only due only to the imprinting features and not the subsequent treatments undergone by the electrode.

2.4. Application of the PAM molecularly imprinted sensor to the samples

Samples (potatoes, potato chips, and bread crust) were purchased from the RT-MART supermarket in June 2013 (WuXi, JiangSu, China). To determine the accuracy of the developed molecularly imprinted sensor, 2.0 g of a potato sample that was verified by HPLC to be free of AM was spiked with 1.0 mL of AM standard solution (0.05, 0.25, and 0.50 mg L^{-1}) in a 100 mL conical flask. After incubation for 1 h, the spiked samples were ultrasonicated with 10 mL methanol for 30 min, and this step was repeated two more times with 10 + 10 mL methanol. The resulting extractants were collected and centrifuged at 4,000 rpm for 30 min, and the supernatants were used for the molecularly imprinted sensor. Samples of potato chips and bread crusts (2.0 g) were extracted and analyzed using the same procedure [31].

3. Result and discussion

3.1. Preparation of imprinted P–ATP–AuNP/Au modified GCE

The whole preparation process for the developed molecularly imprinted sensor is shown in Scheme 1. The preparation procedures can be summarized in four steps: Self-assembly of P–ATP onto the surface of the AuNP/GCE (The characterization of AuNP/GCE is in supporting materials);

Hydrogen bonding adsorption of PAM molecules onto the surface of the P–ATP modified electrode; co-polymerization of the P–ATP–AuNP onto the surface of the PAM/AuNP/GCE; removal of the template propionamide (PAM) molecules from the imprinted P–ATP–AuNP membranes. A large number of tailor–made cavities for acrylamide (AM) formed on the surface of the modified electrode.

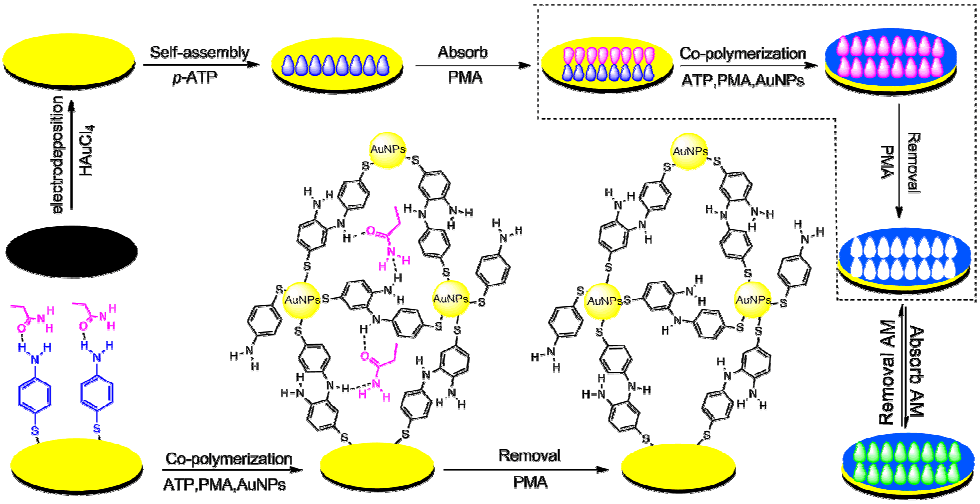

Scheme 1 Molecular imprinting technique

It is of obvious importance that the functional monomers strongly interact with the template and form stable host–guest complexes before polymerization. Considering the properties of PAM and relevant reports, P–ATP can be used as a functional monomer [32, 33]. Before co-polymerization the Au electrode was immersed into a P–ATP solution for 24 h. A self-assembled monolayer of P–ATP molecules was formed on the Au electrode surface by Au–S bonds between gold and the thiol groups (–SH) of P–ATP molecules[32]. In the first step of the electrode modification, the P–ATP monolayer chemisorbed onto the gold electrode surface and exposed an array of amino groups to the solution.

Secondly, the P-ATP/AuNP modified GCE was immersed into a PAM solution for 4 h. The PAM molecules in the solution phase were assembled onto the surface of the P–ATP-modified Au electrode through hydrogen bond interactions between the amino groups ($–NH_2$) of P–ATP and the oxygen atoms of PAM (The intermolecular interaction between PAM and P–ATP studied by UV was showed in Fig. S4). These strong hydrogen bond interactions drive the assembly of PAM molecules onto the surface of the P–ATP modified electrode (Fig. S3 shows the hydrogen-bond interaction between AM, whose analogue is PAM, and p-Aminothiophenol). These ASA molecules that assembled onto the P–ATP modified electrode surface are embedded in the imprinted P–ATP–AuNP membranes and form surface imprinted sites, which increases the amount of imprinted sites on the electrode surface and enhances the sensitivity of the electrode.

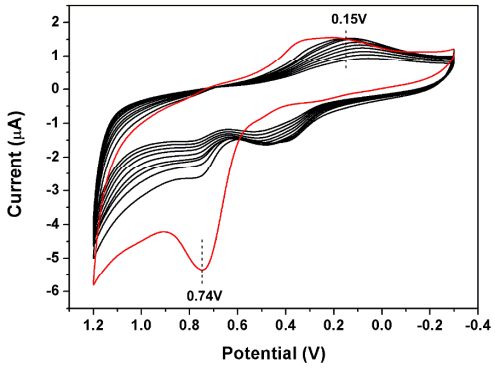

Fig. 1 Cyclic voltammograms for the co-polymerization of 1×10^{-2} mol L^{-1} P–ATP, 1×10^{-2} mol L^{-1} PAM and 5×10^{-2} mol L^{-1} TBAP on the modified GCE in ethanol. Scan rate: 50 mV s^{-1}; number of scans: 10; potential range: −0.3 to 1.2 V.

We improved the one-step co-polymerization method by conducting CVs in a 5 mL ethanol solution containing 1×10^{-2} mol L^{-1} P–ATP, 1×10^{-2} mol L^{-1} PAM and 5×10^{-2} mol L^{-1} TBAP [27]. Figure 1 shows the electrochemical process used to form a P–ATP–AuNP film on a AuNP/GCE (The characterization of the AuNP/GCE is in the supporting materials, Fig. S1 and Fig. S2). The P–ATP–AuNP–PAM film was deposited by repetitively sweeping the potential from −0.2 to 1.2 V at a scan rate of 50 mV s^{-1}. An irreversible oxidation process appeared during the first cycle and disappeared during the second cycle. $HAuCl_4$ was reduced to AuNP and absorbed onto the electrode surface. The Au^3 reduction peak and P–ATP oxidation peak were clearly observed at a potential of about 0.15V and 0.72 V, respectively, in the first scan[27]. The results show that a compact polymeric film was formed and bound to the electrode surface. The decrease in peak current seems to be related to the continuous formation of P–ATP–AuNP composite membranes that leads to the suppression of the voltammetric response (The contact angle experiment of the P-ATP–AuNP/Au modified GCE modified GCE is showed in Fig. S5).

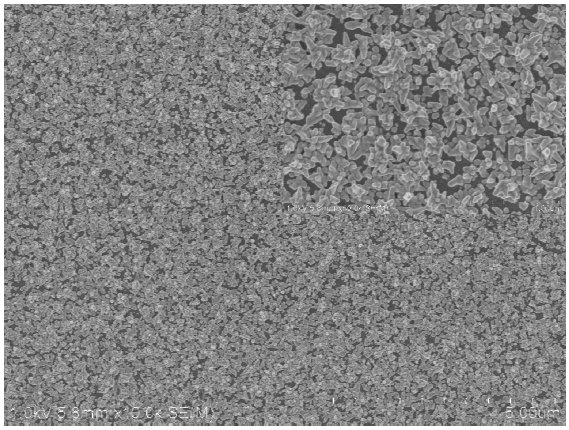

Fig.2. SEM images of the imprinted P-ATP-AuNP membrane formed by five consecutive potential cycles on the modified GCE.

The morphology of the P–ATP/AuNP modified electrode's surface were observed using SEM, as shown in Fig. 2, which is much bigger than the nanoparticles in Fig. S1. The roughness of the P–ATP/AuNP modified electrode's surface increased obviously compared to the surface of the Au electrode indicating that the P–ATP/AuNP co-polymerization resulted in successful coating onto the surface of the electrodes.

3.2. Molecular recognition by the MIP-modified electrode

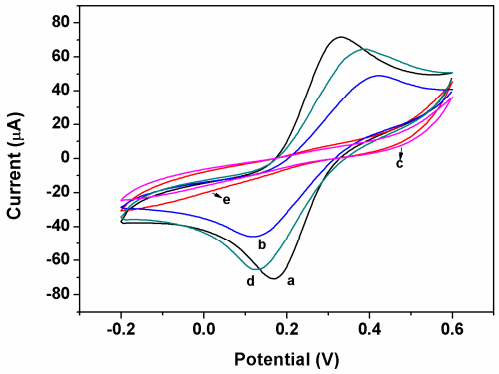

Fig. 3 Cyclic voltammograms of 2.5×10^{-3} mol L^{-1} $[Fe(CN)_6]^{3-}/[Fe(CN)_6]^{4-}$ and 0.1 mol L^{-1} KCl using a Au modified GCE (a), self-assembly of P–ATP on the Au modified GCE (b), MIP-Au modified GCE (c), MIP-Au modified GCE after template removal (d), MIP-Au modified GCE after template rebinding (e), scan rate: 100 mV s^{-1}.

Cyclic voltammograms for the MIP film were recorded in 2.5×10^{-3} mol L^{-1} $[Fe(CN)_6]^{3-}/[Fe(CN)_6]^{4-}$ and 0.1 mol L^{-1} KCl, which was used to confirm whether or not PAM was embedded in the MIP film. During the procedure, $[Fe(CN)_6]^{3-}/[Fe(CN)_6]^{4-}$ was used as a mediator between the imprinted electrodes and substrate solutions. Figure 4 shows the relationship between peak current and surface modification conditions of the Au modified GCE. For the MIP-Au modified GCE, the redox the modified electrode has a high sensitivity for the recognition of PAM. The emergence of curve e is attributed to the limited access of $[Fe(CN)_6]^{3-}/[Fe(CN)_6]^{4-}$ to the MIP film after PAM rebinding. This can be explained by considering the interaction between AM and the MIP film, which determines $[Fe(CN)_6]^{3-}/[Fe(CN)_6]^{4-}$ ion pair electron transfer on the electrode's surface[34, 35].

3.3. Optimization of experimental conditions

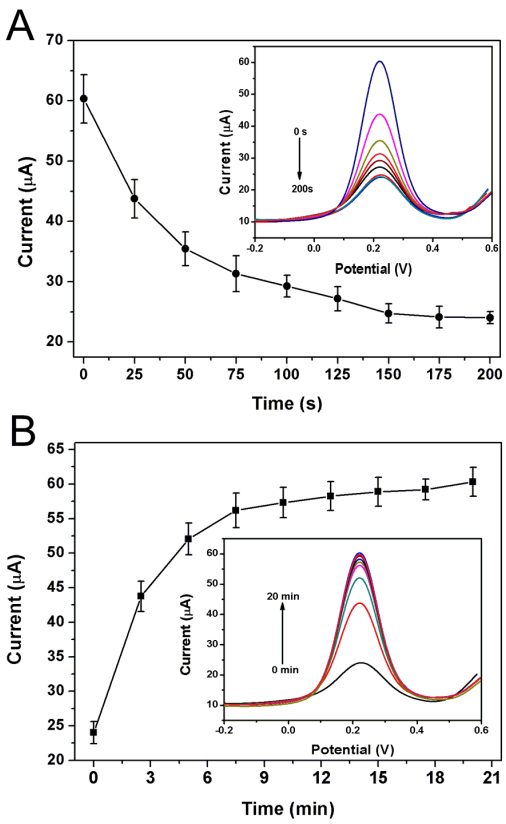

Fig. 4A DPV of the P-ATP–AuNP/Au modified GCE immersed in a 1×10^{-8} mol L^{-1} AM water solution at different times (from 0 to 200 s); Fig. 4B DPV corresponding to the AM–P-ATP–AuNP/Au modified GCE immersed in an ethanol:water (1:5) solution containing 0.5 mol L^{-1} H_2SO_4 at different times (from 0 to 20 min)

The kinetic adsorption of AM onto the MIP sensor is shown in Fig. 4A. The amount of AM adsorbed onto the MIP sensor increased with an increase in adsorption time. We also found that AM is quickly absorbed by the MIP sensor and kinetically the adsorption reaches equilibrium within 150 s. The kinetic curve observed is typical of most rebinding processes, and reveals the rapid dynamic adsorption of AM onto the MIP/Au modified GCE. During the first 150 s, the amount of adsorption increased with adsorption time and after that the amount of adsorption remained constant over time. These results show that the adsorption takes about 150 s to equilibrate.

After electropolymerization, the composite membrane modified electrode was immersed in an ethanol:water (1:5) solution containing 0.5 mol L^{-1} H_2SO_4 to remove the template. As shown in Fig. 4B the current gradually increased and reached a maximum at about 10 min and then remained stable over 10 min, which means that the template was washed out at about 10 min in this solution. As a result, an adsorption time of 150 s and a washing time of 10 min were selected for all subsequent assays.

3.4. Electrochemical detection of AM

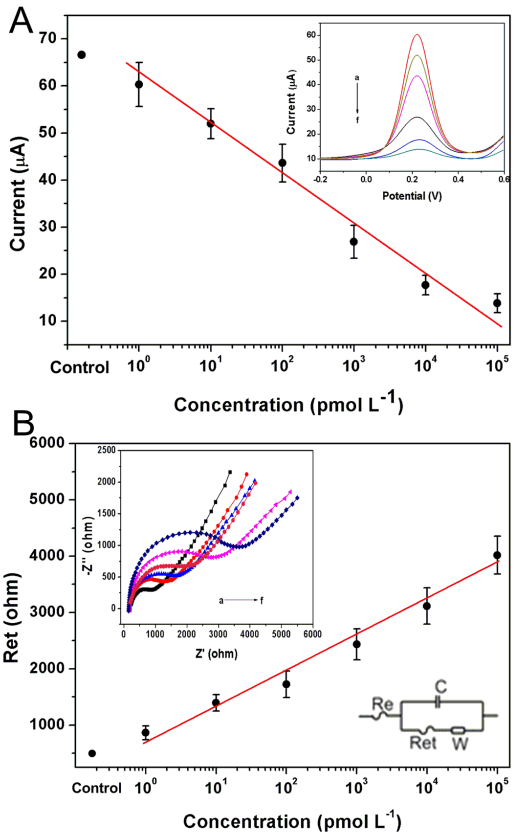

Fig. 5 DPV (A) and EIS (B) of P-ATP-AuNP/Au modified GCE incubated with different concentrations of AM (a-f) 1×10^{-12}, 1×10^{-11}, 1×10^{-10}, 1×10^{-9}, 1×10^{-8}, 1×10^{-7} mol L^{-1} AM in an aqueous solution for 10 min.

For AM detection, the prepared P-ATP–AuNP modified electrodes were immersed in different concentrations of an AM solution (from 1×10^{-12} to 1×10^{-7} mol L^{-1}). When AM adhered to the modified electrode it showed higher charge-transfer impedance and this increase represents the combined effects of a reduction in the DPV current peak value (Fig. 5A) and an increase in the EIS impedance value (Fig. 5B). This shows that when AM is rebound, a compact film appears on the surface of the electrode and this hinders electron transfer from the $[Fe(CN)_6]^{3-}/[Fe(CN)_6]^{4-}$ ion pair to the electrode surface. The formed P-ATP–AuNP–AM complex membrane resulted in a decrease in the electrochemical reaction of the $[Fe(CN)_6]^{3-}/[Fe(CN)_6]^{4-}$ probe.

For the quantitative analysis, the prepared P-ATP–AuNPs/Au modified electrode was incubated using different concentrations of AM for 3 min. DPV and EIS of the MIP film were recorded in a 2.5×10^{-3} mol L^{-1} $[Fe(CN)_6]^{3-}/[Fe(CN)_6]^{4-}$ solution containing 0.1 mol L^{-1} KCl. After 3 min of adsorption the peak current decreased with an increase in the AM concentration because of binding sites in the film being occupied by AM molecules. As shown in Fig. 5A the decrease in DPV signals is directly related to the concentration of AM, which is consistent with the EIS response (Fig. 5B). Two linear relationships exist between the current and the log of AM concentration, and the Ret and the log of the AM concentration from 1×10^{-12} to 1×10^{-7} mol L^{-1} (R

=−0.991 and R = −0.994). A lowest detectable concentration of 5×10^{-13} mol L^{-1} was obtained, which is lower than most available AM detection methods (Table 1).

Table 1 Comparison with other published methods for the determination of AM

Extraction method	Analytical method	Sample type	LOD	Reference
C18 column	LC/MS	fried potato	6.6 μg kg^{-1}	36
MIP/SPE	HPLC	potato chips	0.14 μmol L^{-1}	29
liquid phase extraction	GC/MS	textiles	10 μg kg^{-1}	37
water	cell-based sensor	standard substance	0.1 mmol L^{-1}	38
water	electrochemical sensor	standard substance	0.5 pmol L^{-1}	this work

3.5. Selectivity of the molecularly imprinted sensor

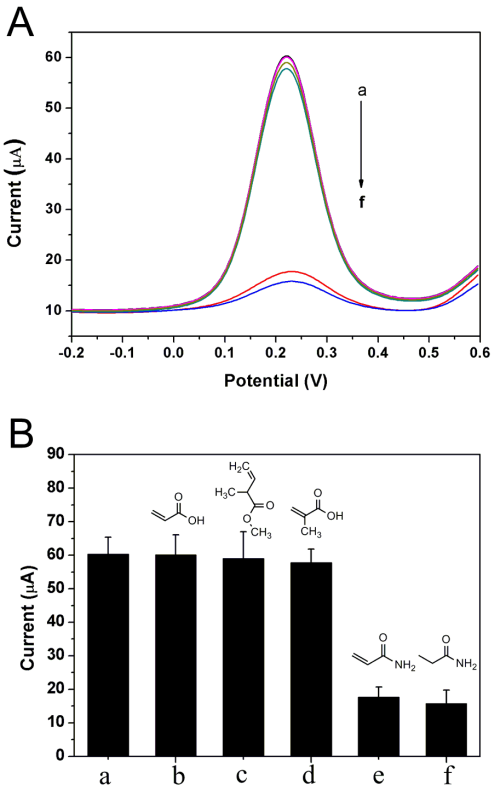

Fig. 6 DPV corresponding to the P-ATP–AuNP/Au modified GCE (a) immersed in 1×10^{-8} mol L^{-1} of a different analogue (b-f): acrylic acid, methacrylamide, methacrylic acid, acrylamide, propionamide.

An excellent sensor not only possesses good sensitivity, but also has good selectivity. To determine the selectivity of the molecularly imprinted sensor we investigated four compounds: acrylic acid, methacrylamide, methacrylic acid and propionamide as control experiments because these have a similar structure to AM. Figure 6 shows different current response signals for the proposed sensing system after the addition of 1×10^{-8} mol L^{-1} acrylic acid, methacrylamide, methacrylic acid and propionamide under the same experimental conditions. The 1×10^{-8} mol L^{-1}

mol L^{-1} AM (e) and propionamide (f) showed a DPV change. However, when ASA was replaced by 1×10^{-8} mol L^{-1} acrylic acid (b), methacrylamide (c), and methacrylic acid (d) the MIP-Au modified GCE hardly changed in terms of its DPV, which proves that the AM molecularly imprinted sensor is highly specific to AM, except in the presence of the dummy template molecule, propionamide.

3.6. Reproducibility and stability

To investigate the reproducibility and repeatability of the MIS, the experiments were performed in 1×10^{-8} mol L^{-1} AM solution. The MIP was expected to be regenerated and the relative standard deviation (RSD) of the peak currents was 3.1 % using three different electrodes. Good repeatability was observed with a RSD of 3.5 % after continuous use for 20 cycles. This revealed that the MIP has good reversibility. The MIP retained 95 % of its original response after 10 d storage at room temperature, and retained 87 % of its original response after 30 d. Furthermore, the response of AM at the MIP hardly changed after 10 min of ultrasonication. All measurements indicated good stability for the MIP.

3.7. Sample analysis

The feasibility of the MIP sensor for practical applications was investigated by analyzing several real samples and comparing with AM results from potatoes purchased from the RT-MART supermarket in June, 2013 (WuXi, JiangSu, China). The potato sample was pretreated as previously reported [31].

Table 2 Average recovery and relative standard deviation of AM (n = 3)

Added concentration (pmol L^{-1})	Detected concentration (pmol L^{-1})	Recovery (%)	R.S.D (%)
100.0	96.8	96.8	3.22
500.0	482.4	96.4	3.73
1000.0	954.7	95.4	2.45

As shown in Table 2, the recovery of AM as detected by the MIP sensor was above 95 %, which means that the MIP sensor possesses an excellent molecular recognition ability, high selectivity, and excellent tolerance. Linear regression shows good linearity with high correlation coefficients ($r > 0.990$). The detection limits and quantification limits were calculated as concentrations to afford a signal that is 3 and 10 times the standard deviation of the baseline noise, respectively. The detection limit was found to be 5×10^{-13} mol L^{-1} (S/N = 3).

4. Conclusions

In this work, a MIP film electrochemical sensor was used to indirectly detect AM. It was constructed and developed by the co-polymerization of P-ATP and $HAuCl_4$ using cyclic voltammetry in the presence of dummy template PAM molecules. PAM molecules absorbed by

hydrogen bonding to the surface of a AuNP modified GCE, which greatly increased the amount of imprinted sites. The doped nanoparticles enhanced the sensitivity of the MIP sensor. In these measurements the lowest detectable concentration of AM was 5×10^{-13} mol L^{-1}, and the linear detection range extended to 1×10^{-7} mol L^{-1}. Furthermore, the fabrication of P–ATP–AuNPs/AuNP/GCE was very simple and controllable, which facilitates a future design of integrated electrodes according to different requirements. These results demonstrate that the electrochemical sensor can significantly improve the sensitivity and selectivity of acrylamide analysis with good repeatability. Therefore, the novel, fast and facile strategy reported here can be used to fabricate various electrochemical sensors for the detection of toxic molecules in food.

Acknowledgments

This work was supported by the ‘‘973’’ National Basic Research Program of China (No. 2012CB720804), the National Rresearch Program (No. 201003008-08, No. 201203069-1), the Program for New Century Excellent Talents in Jiangnan University, and the Priority Academic Program Development of Jiangsu Higher Education Institutions.

5. References

1. S. Belgin Erdoğdu, T. K. Palazoğlu, V. Gökmen, H. Z. Şenyuva and H. I. Ekiz, *Journal of the Science of Food and Agriculture*, 2007, 87, 133-137.
2. A. Dostal, J. Cajdova and H. Hudeckova, *Bratislavské lekárske listy*, 2011, 112, 44.
3. C. A. M. Tas, F. Koster, M. van Tilborg and A. L. L. Duchateau, *Agro Food Ind. Hi-Tech*, 2010, 21, 48-50.
4. Y. Zhang, Z. H. Wen, M. P. Washburn and L. Florens, *Anal. Chem.*, 2011, 83, 9344-9351.
5. I. G. Casella, M. Pierri and M. Contursi, *Journal of Chromatography A*, 2006, 1107, 198-203.
6. C. Li, C. Wang, C. Wang and S. Hu, *Sensors and Actuators B: Chemical*, 2006, 117, 166-171.
7. G. Wulff, *Angewandte Chemie International Edition in English*, 1995, 34, 1812-1832.
8. M.-F. Pan, G.-Z. Fang, B. Liu, K. Qian and S. Wang, *Analytica Chimica Acta*, 2011, 690, 175-181.
9. S. A. Piletsky and A. P. Turner, *Electroanalysis*, 2002, 14, 317-323.
10. M. Blanco-López, M. Lobo-Castanon, A. Miranda-Ordieres and P. Tunon-Blanco, *TrAC Trends in Analytical Chemistry*, 2004, 23, 36-48.
11. O. Y. Henry, A. Fragoso, V. Beni, N. Laboria, J. L. A. Sánchez, D. Latta, F. Von Germar, K. Drese, I. Katakis and C. K. O'Sullivan, *Electrophoresis*, 2009, 30, 3398-3405.
12. F. Farabullini, F. Lucarelli, I. Palchetti, G. Marrazza and M. Mascini, *Biosensors and Bioelectronics*, 2007, 22, 1544-1549.
13. Y. Wang, H. Xu, J. Zhang and G. Li, *Sensors*, 2008, 8, 2043-2081.
14. S. Beutel and S. Henkel, *Applied microbiology and biotechnology*, 2011, 91, 1493-1505.
15. A. Amine, H. Mohammadi, I. Bourais and G. Palleschi, *Biosensors and Bioelectronics*, 2006, 21, 1405-1423.
16. K. Haupt and K. Mosbach, *Chemical Reviews*, 2000, 100, 2495-2504.
17. V. Suryanarayanan, C. T. Wu and K. C. Ho, *Electroanalysis*, 2010, 22, 1795-1811.
18. M. Soleimani, M. G. Afshar, A. Shafaat and G. A. Crespo, *Electroanalysis*, 2013, 25, 1159-1168.
19. S. Hong, L. Y. S. Lee, M. H. So and K. Y. Wong, *Electroanalysis*, 2013, 25, 1085-1094.
20. L. Liu, X. Tan, X. Fang, Y. Sun, F. Lei and Z. Huang, *Electroanalysis*, 2012, 24, 1647-1654.

21. M. B. Gholivand, G. Malekzadeh and M. Torkashvand, *Journal of Electroanalytical Chemistry*, 2013, 692, 9-16.
22. M. Riskin, R. Tel-Vered, T. Bourenko, E. Granot and I. Willner, *Journal of the American Chemical Society*, 2008, 130, 9726-9733.
23. J. Matsui, K. Akamatsu, S. Nishiguchi, D. Miyoshi, H. Nawafune, K. Tamaki and N. Sugimoto, *Analytical chemistry*, 2004, 76, 1310-1315.
24. S. Bharathi, *Anal. Commun.*, 1998, 35, 29-31.
25. C. Li, H. Bai and G. Shi, *Chemical Society Reviews*, 2009, 38, 2397-2409.
26. Y.-J. Liao, Y.-C. Shiang, C.-C. Huang and H.-T. Chang, *Langmuir*, 2012, 28, 8944-8951.
27. Z. Wang, H. Li, J. Chen, Z. Xue, B. Wu and X. Lu, *Talanta*, 2011, 85, 1672-1679.
28. J. Ji, X. Sun, X. Tian, Z. Li and Y. Zhang, *Analytical Letters*, 2013, 46, 969-981.
29. D. Jiang, X. Sun and Y. Zhang, *Anal. Methods*, 2012, 4, 3760-3766.
30. X. Sun, J. Ji, D. Jiang, X. Li, Y. Zhang, Z. Li and Y. Wu, *Biosensors and Bioelectronics*, 2013, 44, 122-126.
31. X. Longhua, Z. Limin, Q. Xuguang, X. Zhixiang and S. Jiaming, *Chromatographia*, 2012, 75, 269-274.
32. C. Xie, H. Li, S. Li, J. Wu and Z. Zhang, *Analytical chemistry*, 2009, 82, 241-249.
33. T. Fodey, P. Leonard, J. O'Mahony, R. O'Kennedy and M. Danaher, *TrAC Trends in Analytical Chemistry*, 2011, 30, 254-269.
34. J. Li, J. Zhao and X. Wei, *Sensors and actuators B: Chemical*, 2009, 140, 663-669.
35. C. Xie, S. Gao, Q. Guo and K. Xu, *Microchimica Acta*, 2010, 169, 145-152.
36. M. Jezussek and P. Schieberle, *Journal of agricultural and food chemistry*, 2003, 51, 7866-7871.
37. J. Jin, W. Dong and Y. Liang, *AATCC Rev.*, 2013, 13, 58-63.
38. X. Sun, J. Ji, D. Jiang, X. Li, Y. Zhang, Z. Li and Y. Wu, *Biosensors and Bioelectronics*, 2013.